LA-UR 89-3337

Conf-8906237--1

Los Alamos National Laboratory is operated by the University of California for the United States Department of Energy under contract W-7405-ENG-36

LA-UR--89-3337

DE90 002437

TITLE HAMILTONIAN CHAOS IN A NONLINEAR POLARIZED OPTICAL BEAM

AUTHOR(S) D. David, D. D. Holm, and M. V. Tratnik

SUBMITTED TO Submitted to the Proceedings of the Santa Fe Institute Summer School on Complex Systems, held June 5-30, 1989

DISCLAIMER

MASTER

Los Alamos Los Alamos National Laboratory
Los Alamos, New Mexico 87545

HAMILTONIAN CHAOS IN A NONLINEAR POLARIZED OPTICAL BEAM

D. David, D.D. Holm, and M.V. Tratnik
C.N.L.S. and Theoretical Division, MS B258
Los Alamos National Laboratory
Los Alamos, NM 87545

Abstract. This lecture concerns the applications of ideas about temporal complexity in Hamiltonian systems to the dynamics of an optical laser beam with arbitrary polarization propagating as a travelling wave in a medium with cubically nonlinear polarizability. We use methods from the theory of Hamiltonian systems with symmetry to study the geometry of phase space for this optical problem, transforming from C^2 to $S^3 \times S^1$, first, and then to $S^2 \times (J, \theta)$, where (J, θ) is a symplectic action-angle pair. The bifurcations of the phase portraits of the Hamiltonian motion on S^2 are classified and displayed graphically. These bifurcations take place when either J (the beam intensity), or the optical parameters of the medium are varied. After this bifurcation analysis has shown the existence of various saddle connections on S^2, the Melnikov method is used to demonstrate analytically that the travelling-wave dynamics of a polarized optical laser pulse develops chaotic behavior in the form of Smale horseshoes when propagating through spatially periodic perturbations in the optical parameters of the medium.

1. Introduction. Hamiltonian dynamics often produces temporal complexity when regular, integrable motion undergoes small periodic perturbations. The presence of such complexity in perturbed Hamiltonian systems was first encountered by Poincaré in his study of the Newtonian three-body problem. Hamiltonian complexity is also one of the most important implications of the celebrated Kolmogorov-Arnold-Moser (KAM) theorem.

Complexity arising from periodic perturbations of integrable Hamiltonian systems usually appears as horseshoe chaos, and is characterized as the limit set of intersections of phase space regions resulting from iterating the Smale horseshoe map. In two dimensions, this map first stretches and folds a rectangular region in phase space into a horseshoe shape of the same area; next the map overlays the horseshoe onto the original rectangle and then takes the intersection. Iterating the map repeats this stretching and folding process recursively: the two rectangular regions comprising the intersection of the first horseshoe with the original region iterate under the map to make four regions of intersection, iterate again to make eight, and so forth. In the limit, the horseshoe map iterates to produce

an invariant Cantor-like set, i.e., a fractal set in phase space, called a Smale horseshoe. The dynamics of the horseshoe map on its invariant set can be associated to symbolic shifts. Such shifts produce sensitive dependence on initial conditions, which is a hallmark of chaos. To see intuitively how this sensitive dependence on initial conditions arises from the association of the dynamics of the horseshoe map to symbolic shifts, think of each initial condition as the fractional part of a binary number. An iteration of the horseshoe map corresponds to taking the fractional part of the binary number obtained from the initial one by shifting the "decimal point" one place to the right. Thus, after n iterations the subsequent motion depends on details of the initial condition from beyond its n-th significant figure!

For the periodically perturbed Hamiltonian system considered in this lecture, the Smale horseshoe map is obtained from the Poincaré map, here the time T map of the perturbed phase space orbit, where T is the period of the perturbation. A method due to Melnikov [1963] and Arnold [1964], and developed further by Holmes and Marsden [1982] and Wiggins [1988], is used to establish analytically that iterating the Poincaré map for the perturbed system produces transverse intersections of stable and unstable manifolds of perturbed homoclinic points. Each transverse intersection is an unstable homoclinic point of the perturbed Poincaré map and is an unstable periodic orbit of the perturbed system. The Poincaré-Birkhoff-Smale homoclinic theorem is then invoked to assert the existence, near any perturbed transverse homoclinic point, of an invariant Cantor-like set on which some power of the Poincaré map for the perturbed system corresponds to a shift on two symbols, thereby implicating the Smale horseshoe map as the mechanism for chaos.

In using the Melnikov-Arnold method, transverse intersections are shown to exist by establishing for each homoclinic point of the unperturbed system that the (signed) distance in first order perturbation theory between its stable and unstable manifolds develops simple zeroes under perturbation. (Under small enough perturbations the original homoclinic point displaces slightly, but it continues to exist as a hyperbolic critical point.) Thus, establishing the zeroes of this signed distance (which is usually called the Melnikov function) allows one to conclude that the Poincaré map for the perturbed problem contains the stretching, folding, and intersecting processes necessary to produce horseshoe chaos. There are an infinite number of these zeroes of the Melnikov function for the perturbed Poincaré map, and each one corresponds to a transverse intersection of the stable and unstable man

ifolds of the perturbed homoclinic point. In turn, each of these intersections corresponds to an unstable periodic orbit, around which further transverse intersections can develop in principle, resulting in exquisitely complex dynamics even for perturbed Hamiltonian systems in only two dimensions plus time (one and a half degrees of freedom).

For higher degrees of freedom, resonance overlaps and Arnold webs can develop, leading to even richer complexity in higher dimensions. While horseshoes and their higher-dimensional counterparts are not strange attractors (since we are dealing only with Hamiltonian systems here), they do have quantifiable mixing and transport properties, and they often behave like strange attractors in numerical simulations (perhaps because of dissipation and noise due to round-off). The investigation of these features (especially in higher dimensions) is one of the great challenges of modern science. See Wiggins [1988] for further explanations and examples of horseshoe chaos, as well as references and discussions concerning the original mathematical development of this field.

The complex dynamics we discuss in this lecture appears in a physical application concerning the Hamiltonian description of the travelling-wave dynamics of a polarized, nearly monochromatic, optical laser pulse propagating in a lossless, cubically nonlinear, parity-invariant, anisotropic, homogeneous medium (for instance, a polarized beam in a straight optical fiber). Our approach combines methods of reduction of phase space dimension for Hamiltonian systems possessing continuous symmetry groups together with the method of Arnold and Melnikov for showing the existence of complex behavior under small perturbations of integrable dynamical systems. This approach provides a unified and geometrical view of the qualitative properties of polarization dynamics (e.g., phase portraits, bifurcations, and special solutions), while at the same time showing that this physical application possesses complex dynamics under conservative spatially-periodic perturbations of the optical parameters of the medium.

Nonlinear polarization dynamics of optical laser pulses has been studied for about three decades, almost since the invention of the laser. Maker *et al.* [1964] demonstrated the precession of the polarization ellipse for a single beam propagating in a nonlinear medium. Stable solutions for the problem of two counterpropagating beams were examined in Kaplan [1983] and Lytel [1984]. Studies of polarization bistability in isotropoic media and computer simulations suggesting chaotic behavior can be found in Otsuka *et al.* [1985] and Gaeta *et al.* [1987]. Previous work on special solutions of both the one beam and the

two–beam problems appear in Tratnik and Sipe [1987]. For additional references and more detailed treatments of Hamiltonian chaos in nonlinear optical polarization dynamics, see David, Holm, and Tratnik [1988a, 1988b, 1989] and David [1989].

The plan of the lecture is as follows. In Section 2 we cast polarization dynamics for travelling–wave optical pulses into Hamiltonian form in terms of two complex electric field amplitudes, one amplitude for each polarization in the plane transverse to the direction of propagation. In Section 3 we use the method of reduction for Hamiltonian systems with symmetry to transform to the Stokes representation of polarization dynamics. Invariance of the polarization dynamics Hamiltonian under simultaneous changes of phase of the two complex electric field amplitudes leads to conservation of an action variable, J, conjugate to the phase angle, θ. This action variable is the total light intensity (i.e., the sum of the squares of the amplitudes of the two linear polarizations). We perform the reduction process in two steps: from C^2 to $S^3 \times S^1$, first, and then to $S^2 \times (J, \theta)$. The first reduction gives a geometric picture of the dynamics as taking place along intersections of level surfaces of constants of motion in S^3, while the second reduction gives phase space portraits on the spherical surface, S^2. In Section 4 we classify the various fixed points of the reduced dynamics and describe the bifurcations which take place as the material parameters and intensity of the light are varied. On S^2 we find saddle points connected among themselves by heteroclinic and homoclinic orbits. For the particular case of an optically active isotropic medium, we present the complete bifurcation diagram depicting how the heteroclinic and homoclinic orbits reconnect among themselves as the beam intensity is varied. In Section 5 we use the Melnikov method to demonstrate how these orbits tangle and break up into stochastic layers characterized by Smale horseshoes under perturbations of the travelling–wave dynamics caused by material inhomogeneities, modelled as spatially periodic variations of the optical parameters of the medium. The conclusions of this study are summarized in Section 6.

2. Physical formulation of the problem. Travelling–wave polarization dynamics is expressed in terms of complex electric field amplitudes $e_i(\tau)$, appearing in the following eikonal expression for the electric field,

$$E_i(\tau) = e_i(\tau)e^{i(kz-\omega t)} + e_i^*(\tau)e^{-i(kz-\omega t)} \qquad (2.1)$$

where $\tau = z - ct$ is the travelling-wave variable and where $i = 1, 2$ is the polarization index. The third-order nonlinear polarizability is written as

$$P_i(z,t) = \chi * E_i + \chi^{(1)}_{ij} * E_j + \chi^{(3)}_{ijk\ell} * E_j E_k E_\ell \tag{2.2}$$

where $*$ indicates convolution with respect to time and we sum over repeated indices. Using the rotating wave approximation in Maxwell's equations and assuming we are far from resonances leads to the following equations of travelling-wave motion for the slowly varying amplitudes

$$i\frac{de_j}{d\tau} = \chi^{(1)}_{jk} e_k + 3\chi^{(3)}_{jk\ell m} e_k e_\ell e^*_m. \tag{2.3}$$

where the constant susceptibility tensors $\chi^{(1)}$ and $\chi^{(3)}$ satisfy the following involutions:

$$\chi^{(1)}_{ij} = \chi^{(1)*}_{ji}, \qquad \chi^{(3)}_{ijk\ell} = \chi^{(3)*}_{ji\ell k}, \qquad \chi^{(3)}_{ijk\ell} = \chi^{(3)}_{\ell jki} = \chi^{(3)}_{ikj\ell}. \tag{2.4}$$

These equations constitute a Hamiltonian system on C^2 with Hamiltonian function

$$H = e^*_j \chi^{(1)}_{jk} e_k + \tfrac{3}{2} e^*_j e_k \chi^{(3)}_{jk\ell m} e_\ell e^*_m \tag{2.5}$$

and Poisson bracket

$$\{F, G\} = i\left(\frac{\partial F}{\partial e^*_j}\frac{\partial G}{\partial e_j} - \frac{\partial F}{\partial e_j}\frac{\partial G}{\partial e^*_j}\right) \tag{2.6}$$

so that any dynamical quantity Q evolves according to the prescription

$$\frac{dQ}{d\tau} = \{Q, H\}. \tag{2.7}$$

3. Reduction to S^2. In general, Hamiltonian systems endowed with continuous symmetries are reducible in the sense that they may be written in terms of fewer variables by making use of the conservation laws associated with these symmetries. For the system (2.3) under consideration here, the Hamiltonian function H in (2.5) is invariant under an S^1 action. That is, H remains unchanged under the transformation $\mathbf{e} \mapsto e^{i\theta}\mathbf{e}$; so it is natural to transform to invariant coordinates, as follows:

$$\mathbf{u} = \mathbf{e}^\dagger \vec{\sigma} \mathbf{e}, \qquad u_0 \equiv r = \mathbf{e}^\dagger \cdot \mathbf{e}, \tag{3.1}$$

where $\vec{\sigma} = (\sigma_3, \sigma_1, \sigma_2)$ are the usual Pauli matrices. In terms of these invariant variables, also known as the *Stokes parameters*, the equations of motion become

$$\frac{d\mathbf{u}}{d\tau} = (\mathbf{b} + \mathbf{W} \cdot \mathbf{u}) \times \mathbf{u}, \tag{3.2}$$

where

$$\mathbf{b} = \mathbf{a} + r\mathbf{c}, \tag{3.3a}$$

$$\mathbf{a} = \vec{\sigma}_{ij}\chi^{(1)}_{ji}, \qquad \mathbf{c} = \tfrac{4}{3}\vec{\sigma}_{ij}\chi^{(3)}_{jikk}, \tag{3.3b}$$

$$\mathbf{W} = \vec{\sigma}_{ij}\chi^{(3)}_{ijk\ell}\vec{\sigma}_{k\ell} = \mathrm{Diag}\,(\lambda_1, \lambda_2, \lambda_3)\,, \tag{3.3c}$$

with Hamiltonian function in the new variables

$$H = \mathbf{b} \cdot \mathbf{u} + \tfrac{1}{2}\mathbf{u} \cdot \mathbf{W} \cdot \mathbf{u}, \tag{3.4}$$

and Poisson bracket

$$\{F, G\} = \mathbf{u} \cdot \frac{\partial F}{\partial \mathbf{u}} \times \frac{\partial G}{\partial \mathbf{u}} \tag{3.5}$$

in terms of which equations (3.2) can be reexpressed as

$$\frac{d\mathbf{u}}{d\tau} = \{\mathbf{u}, H\} = \frac{\partial H}{\partial \mathbf{u}} \times \mathbf{u}. \tag{3.6}$$

The quantities a_1, a_3, c_1, c_3 are birefringence terms, and a_2, c_2 are optical activity terms; **a** and **c** refer to linear and induced effects, respectively. The components of **W** are interaction terms of the following types: W_{11}, W_{13}, W_{33} are linear–linear polarization interaction terms, W_{12}, W_{23} are linear–circular polarization interaction terms, and W_{22} is a circular–circular polarization interaction term. A few comments are now in order. First, we observe that the equations of motion (3.2), or equivalently (3.6), are those for a rigid body with a flywheel attachment. Similarities with rigid bodies will be clear in the next section when we will examine the geometry of the phase portrait for the system. Second, it is to be noted that u_0, or r, is a constant function; it in fact is a *Casimir function*, i.e., it commutes with any function for which the Poisson bracket (3.5) is well defined. The quantity r being a constant means that it is dynamically irrelevant, since it is fixed once initial conditions have been specified. When such symmetries occur due to invariance under a continuous group, it proves natural to transform to more appropriate coordinate functions in order to reparametrize the original system into a lower dimensional one. Here, the transformation (3.1) to invariant coordinates is the natural choice and the geometry of the *reduced manifold*

is that of the hypersphere S^3. In this connection, we mention that (3.1) is a well known transformation. Indeed, let us express the complex components of the electric field as

$$\mathbf{e} = (e_1, e_2) = (x_1 + ix_2, x_3 + ix_4). \tag{3.8}$$

Then (3.1) can be rewritten as

$$u_0 = x_1^2 + x_2^2 + x_3^2 + x_4^2, \tag{3.9a}$$

$$u_3 = 2(x_1x_3 + x_2x_4), \tag{3.9b}$$

$$u_1 = 2(x_1x_4 - x_2x_3), \tag{3.9c}$$

$$u_2 = x_1^2 + x_2^2 - x_3^2 - x_4^2. \tag{3.9d}$$

The **u** part, i.e., (3.9b-d), is the transformation $S^3 \mapsto S^2$ due to Hopf (see, e.g., Crampin and Pirani [1987]). We must point out that the components **u** are not all independent; indeed,

$$u_1^2 + u_2^2 + u_3^2 = r^2. \tag{3.10}$$

Thus, we really are dealing with a two-dimensional manifold, the sphere S^2 in view of (3.10). We will reduce to S^2 momentarily. The two-dimensional sphere (3.10) is sometimes referred to as the *Poincaré sphere* (see Figure 3.1). Points on this sphere represent polarization states: the poles are circularly polarized states, equatorial points correspond to linearly polarized states, and all other points describe elliptical states. We are choosing the north and south poles to lie along the 2-axis to conform with optics notation.

Another point deserves attention here. We observe that the Poisson bracket (3.5) and the dynamical equations (3.6) can also be written as

$$\{F, G\} = \frac{\partial K}{\partial \mathbf{u}} \cdot \frac{\partial F}{\partial \mathbf{u}} \times \frac{\partial G}{\partial \mathbf{u}}, \tag{3.11a}$$

$$\frac{d\mathbf{u}}{d\tau} = \{\mathbf{u}, H\} = \frac{\partial H}{\partial \mathbf{u}} \times \frac{\partial K}{\partial \mathbf{u}}, \tag{3.11b}$$

where

$$K = \tfrac{1}{2}|\mathbf{u}|^2. \tag{3.11c}$$

Equation (3.11b) indicates that the motion in the Euclidean three-space takes place along the intersection of the level surfaces of the functions K, a sphere of radius r, and H,

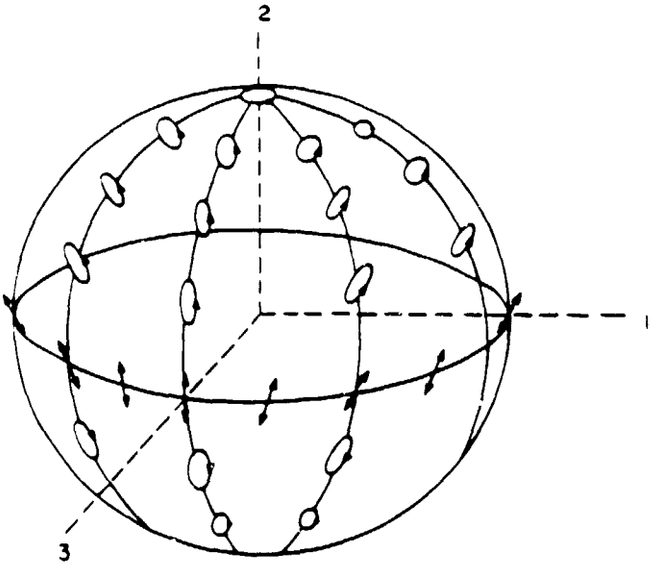

Figure 3.1. The Poincaré sphere.

a quadric surface. Fixed points for the system occur when the level surfaces of H and K are tangent. The Poisson bracket in (3.11a) satisfies the Jacobi identity for every (differentiable) function K. When restricted to a level surface of K the Poisson bracket becomes symplectic. Such a restriction is always possible because K is a Casimir function for the Poisson bracket (3.11a), i.e., $\{K, H\} = 0$ for every choice of H. One also observes that these spheres form a *symplectic foliation* of S^3; the *symplectic leaves* are the spheres of radii r.

In the present case, we restrict to the sphere S^2 by using the usual transformation to spherical coordinates:

$$\mathbf{u} = (u_1, u_2, u_3) \mapsto (r \sin\theta \sin\phi, r \cos\theta, r \sin\theta \cos\phi) \tag{3.12}$$

In terms of these coordinates, the Hamiltonian function, the Poisson bracket, and the equations of motion take the following symplectic form:

$$H = \tfrac{1}{2}r^2\left[(\lambda_1 \sin^2\phi + \lambda_3 \cos^2\phi)\sin^2\theta + \lambda_2 \cos^2\theta\right] \qquad (3.13)$$
$$+ r\sin\theta(b_1 \sin\phi + b_3 \cos\phi) + b_2 r\cos\theta\ ,$$

$$\{F, G\} = \frac{1}{r}\left(\frac{\partial F}{\partial \phi}\frac{\partial G}{\partial \cos\theta} - \frac{\partial G}{\partial \phi}\frac{\partial F}{\partial \cos\theta}\right)\ , \qquad (3.14)$$

$$\frac{d\theta}{d\tau} = b_1 \cos\phi - b_3 \sin\phi + (\lambda_1 - \lambda_3)\, r\sin\theta\cos\phi\sin\phi\ , \qquad (3.15a)$$

$$\frac{d\phi}{d\tau} = b_2 - (b_1 \sin\phi + b_3 \cos\phi)\cot\theta - r\left(\lambda_1 \sin^2\phi + \lambda_3 \cos^2\phi - \lambda_2\right)\cos\theta\ . \qquad (3.15b)$$

Before studying the qualitative aspects of equations (3.15), let us present some special cases which reduce to the well known ***Duffing oscillator***. First, consider the case when $\mathbf{W}$ is of the form $\mathbf{W} = \omega\mathrm{Diag}(1,1,2)$ with $\mathbf{b} = (b_1, b_2, 0)$. Eliminating u_1 and u_2 from the equations of motion for u_3 yields the following Duffing equation:

$$\frac{d^2u_3}{d\tau^2} = Au_3\left(B - u_3^2\right), \qquad (3.16a)$$

$$A = \tfrac{1}{2}\omega^2, \qquad B = \frac{2H}{\omega} - r^2 - \frac{2\left(b_1^2 + b_2^2\right)}{\omega^2}. \qquad (3.16b)$$

When B passes through zero, the solutions undergo a ***pitchfork*** bifurcation and develop *homoclinic* orbits. As a second example, let $\mathbf{W}$ be as above and $\mathbf{b} = (b_1, 0, b_3)$. Eliminating as in the previous case again yields a Duffing equation:

$$\frac{d^2u_3}{d\tau^2} = A + Bu_3 + Cu_3^2 + Du_3^3, \qquad (3.17a)$$

$$A = b_3\left(H - \tfrac{1}{2}\omega r^2\right), \qquad C = -\tfrac{1}{2}\omega b_3, \qquad (3.17b)$$

$$B = \omega H - \tfrac{1}{2}\omega^2 r^2 - b_1^2 - b_3^2, \qquad D = -\tfrac{1}{2}\omega^2. \qquad (3.17c)$$

Here, the poiarization dynamics reduces to the motion of a particle in a one–dimensional quartic potential well and has solutions expressible in terms of elliptic functions. Chaotic response to perturbations of the Duffing oscillator are studied in Greenspan and Holmes [1981] and in Wiggins [1988]

4. Phase portrait analysis. In this section, we will investigate the nature of the phase portrait for the reduced system (3.15). Specifically, we wish to determine the fixed points and determine their type; since we are dealing with a Hamiltonian system, the fixed points can only be stable *centers* or unstable *saddle points*, although some exotic points may arise as *pseudo critical points* when degenerate bifurcations take place.

The generic form of (3.15) contains six parameters and prevents any easy analysis; we will therefore proceed by examining a sequence of increasingly complex subcases. It turns out that the following list provides an exhaustive division into inequivalent subcases (see Tratnik and Sipe [1987]):

$$\begin{array}{lll}
\text{Case 1.} & \mathbf{b} = (0,0,0)\,, & \mathbf{W} = \mathrm{diag}(\lambda_1,\lambda_2,\lambda_1)\ ; \\
\text{Case 2.} & \mathbf{b} = (0,0,0)\,, & \mathbf{W} = \mathrm{diag}(\lambda_1,\lambda_2,\lambda_3)\ ; \\
\text{Case 3.} & \mathbf{b} = (0,b_2,0)\,, & \mathbf{W} = \mathrm{diag}(\lambda_1,\lambda_2,\lambda_1)\ ; \\
\text{Case 4.} & \mathbf{b} = (0,b_2,0)\,, & \mathbf{W} = \mathrm{diag}(\lambda_1,\lambda_2,\lambda_3)\ ; \\
\text{Case 5.} & \mathbf{b} = (b_1,0,b_3)\,, & \mathbf{W} = \mathrm{diag}(\lambda_1,\lambda_2,\lambda_3)\ ; \\
\text{Case 6.} & \mathbf{b} = (b_1,b_2,b_3)\,, & \mathbf{W} = \mathrm{diag}\ (\lambda_1,\lambda_2,\lambda_3)\ .
\end{array} \tag{4.1}$$

Parity-invariant optical media are characterized by $b_2 = 0$. For more details concerning the results presented here, see David, Holm, and Tratnik [1989]; Case 4, including small dissipation and driving, is exhaustively analyzed in David [1989].

Cases 1 and 2 $\mathbf{b} = (0,0,0)$, $\mathbf{W} = \mathrm{Diag}(\lambda_1,\lambda_2,\lambda_3)$. The phase portrait is function of a single parameter, $M = \lambda_3/\lambda_1$. Case 1 is thus obtained as the limit $M \to 1$. Figure 4.1 shows the phase portraits for various values of M. This case is exactly that of the rigid body, as clearly indicated by the equations of motion (3.2) when $\mathbf{b} = 0$. In particular, note that for case 1 the motion reduces to latitudinal circular orbits, which tells us that the polarization ellipse just undergoes precession about the circular state. In case 2 the phase portraits are characterized by four centers and 2 saddle points connecting four *heteroclinic* orbits. Exceptions occur when $M = 0, 1, \pm\infty$: the heteroclinic orbits then merge pairwise to form invariant great circles of fixed points.

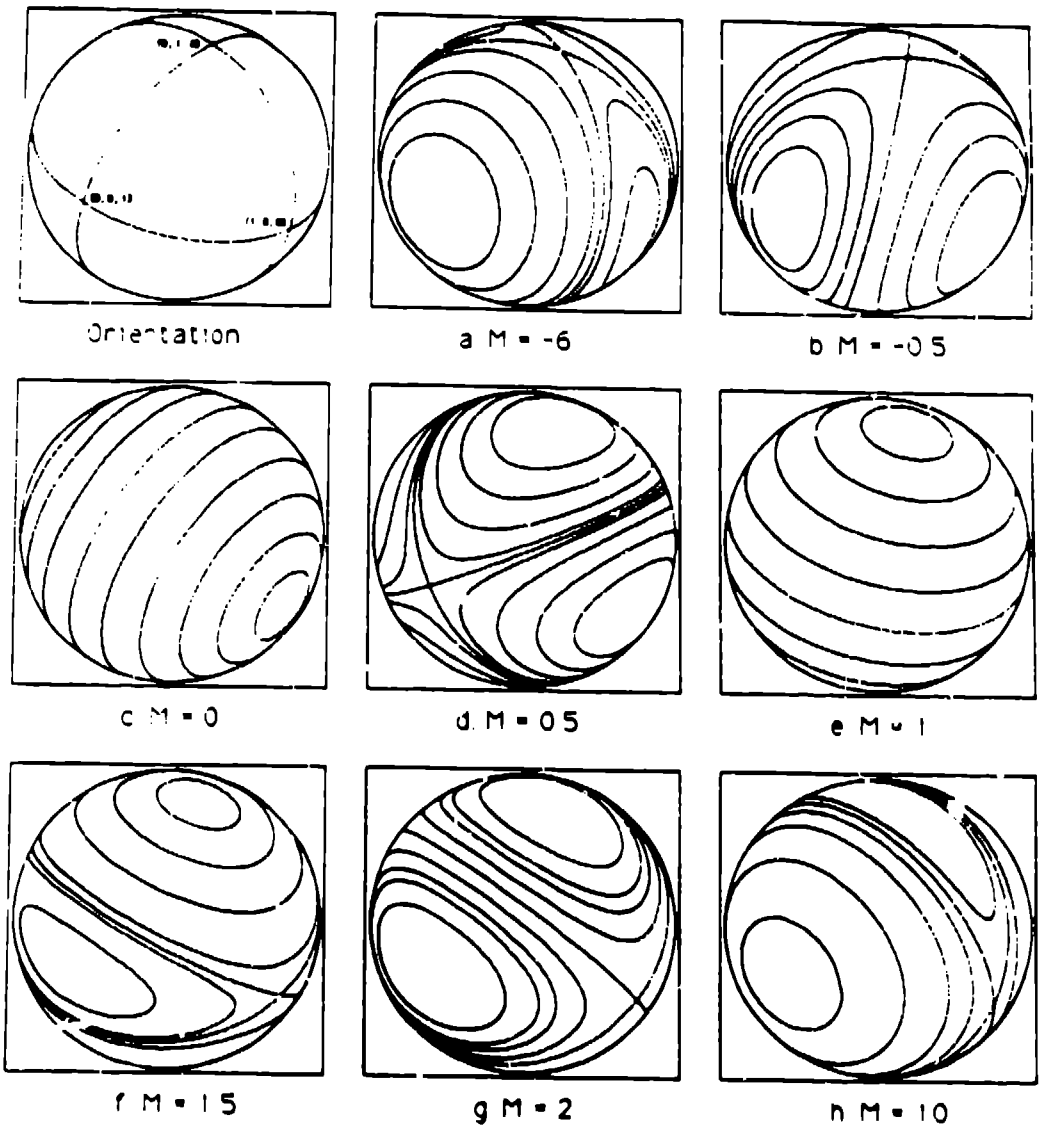

Figure 4.1. The phase portrait for cases 1 and 2 similar to that of the rigid body.

Cases 3 and 4 $\mathbf{b} = (0, b_2, 0)$, $\mathbf{W} = \mathrm{Diag}(\lambda_1, \lambda_2, \lambda_3)$. These cases are characterized by two independent parameters, which we write as

$$\lambda = \frac{(\lambda_2 - \lambda_1)}{(\lambda_3 - \lambda_1)}, \qquad \beta = \frac{b_2}{r(\lambda_3 - \lambda_1)}. \tag{4.2}$$

Case 3 is recovered in the limit $\lambda \to \infty$, $\beta \to \infty$. In this case, we see that the right-hand side of (3.15a) identically vanishes; we then deduce that poles are stable points and that there exists a circle of fixed points determined by $\cos\theta = b_2/r(\lambda_2 - \lambda_1) = \beta/\lambda$. The fixed points of equations (3.15) are quite easily determined and classified by using the *energy*-

Casimir stability technique (see Holm *et al.* [1985]); we list the results in the following table.

Fixed Point	Coordinates	Constraint	Saddle	Center
F	$\phi = 0 \quad \cos\theta = \beta/(1-\lambda)$	$\beta^2 < (1-\lambda)^2$	$\lambda > 1$	$\lambda < 1$
B	$\phi = \pi \quad \cos\theta = \beta/(1-\lambda)$			
L	$\phi = \pi/2 \quad \cos\theta = -\beta/\lambda$	$\beta^2 < \lambda^2$	$\lambda < 0$	$\lambda > 0$
R	$\phi = -\pi/2 \quad \cos\theta = -\beta/\lambda$			
N	$\cos^2\phi = \lambda + \beta \quad \theta = 0$	———	$0 < \lambda + \beta < 1$	$\lambda + \beta \notin (0,1)$
S	$\cos^2\phi = \lambda - \beta \quad \theta = \pi$	———	$0 < \lambda - \beta < 1$	$\lambda - \beta \notin (0,1)$

Table. The fixed points of system (3.12) and their types.

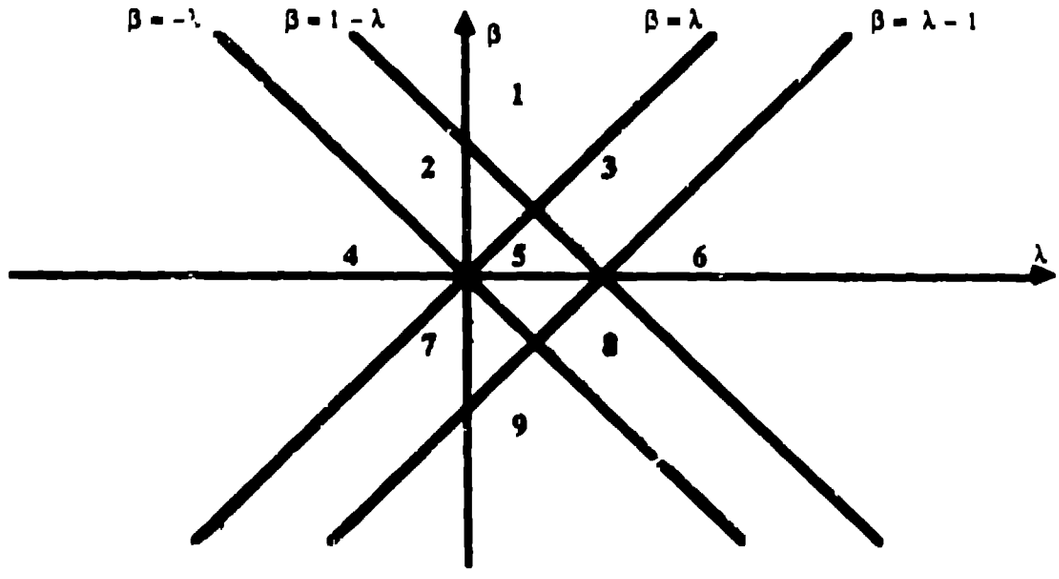

Figure 4.2 The parameter plane for case 4.

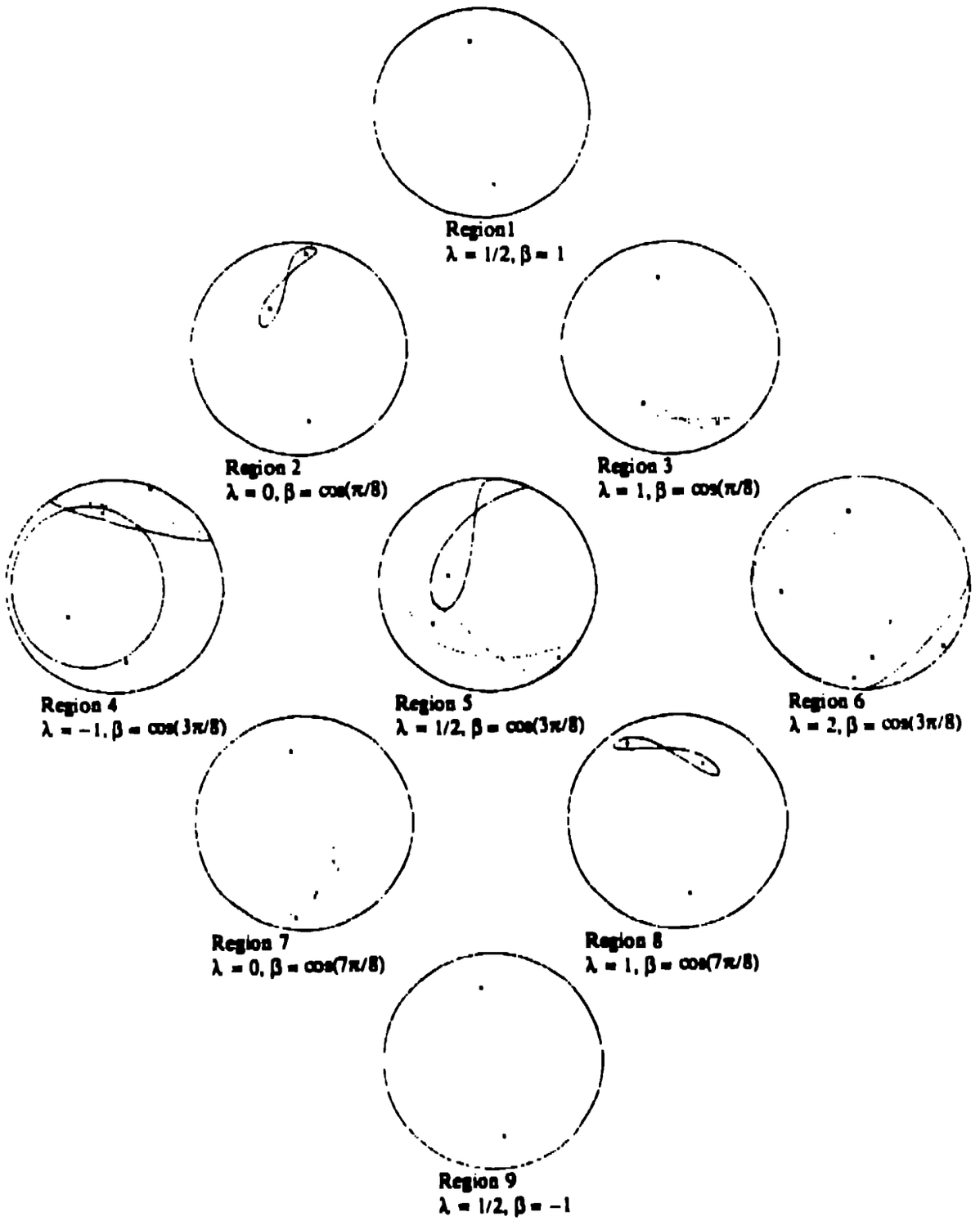

Figure 4.3. Phase portraits for case 4.

Bifurcations take place when the inequalities in the above table become equalities; thus, the pairs of fixed points (F,B) and (L,R) appear or vanish as the lines $\beta = \pm(1-\lambda)$ and $\beta = \pm\lambda$ are traversed in the parameter plane, respectively (see Figure 4.2). This plane is divided into nine distinct regions separated by four critical lines that intersect at four points. The phase portraits corresponding to points within the various regions are depicted in Figure 4.3. The λ-axis, i.e., $\beta = 0$, is a special line. Along this line, we recover the equations of motion for the rigid body since $\beta = 0$ essentially yields case 3 as a subcase. For points on the λ-axis, the corresponding phase portraits are also special. For instance, consider region 5. The phase portrait there consists of saddle points at the poles, each of which being connected to a pair of homoclinic orbits. When β goes to zero these two pairs of loops merge to form four heteroclinic orbits. Variations of beam intensity correspond to moving along vertical lines in the λ-β plane. A Hamiltonian pitchfork bifurcation takes place whenever one of the four critical lines is crossed from one region of this plane to another.

For the remaining two cases in (4.1), our analysis of the phase portraits is still incomplete in view of the complexity of the stability conditions for the fixed points; the full results will be presented elsewhere upon completion. We will nevertheless show typical pictures exemplifying the phase space configuration for each of these cases.

Case 5 $\mathbf{b} = (b_1, 0, b_3)$, $\mathbf{W} = \mathrm{Diag}(\lambda_1, \lambda_2, \lambda_3)$. For this case, there are three independent bifurcation parameters. The phase portrait consists of at least two and up to six fixed points. The stability criteria for these fixed points are quite complicated expressions and will not be presented here. This case has a new feature, namely tangent bifurcations, in which a saddle–center pair combines into a cusp, which then smoothens into a regular orbit as the bifurcation parameter passes through a critical value. In Figure 4.4, we illustrate a typical set of phase portraits for this case; we set $b_1 = b_3 = -1$, $\lambda_1 = 1$, $\lambda_2 = 0$, and we vary $M = \lambda_3$. In particular, observe the tangent bifurcation occuring in Figure 4.4*k*.

Case 6 $\mathbf{b} = (b_1, b_2, b_3)$, $\mathbf{W} = \mathrm{Diag}(\lambda_1, \lambda_2, \lambda_3)$. This is the general case for which there are four independent bifurcation parameters; the structure of the phase space for the full system can therefore be quite complex. Here again, there may be up to six fixed points for the system and the stability conditions are very complicated. Not unexpectedly, this case also features tangent bifurcations. Figure 4.5 illustrates phase portraits for this case; for

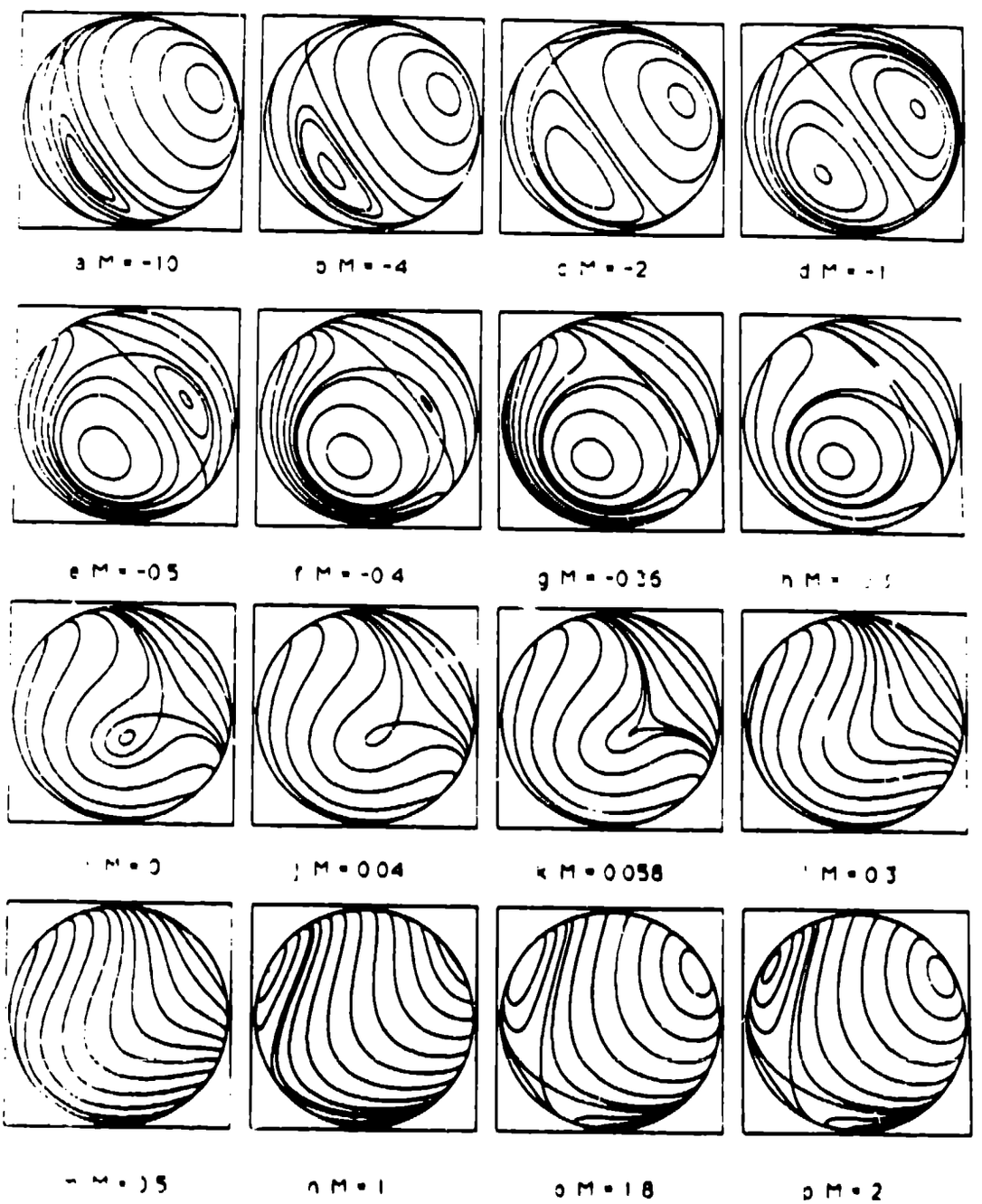

Figure 4.4. Bifurcations for case 5.

the pictures therein, we have chosen the same parameter values as for the previous case and, in addition, $J_2 = -2$.

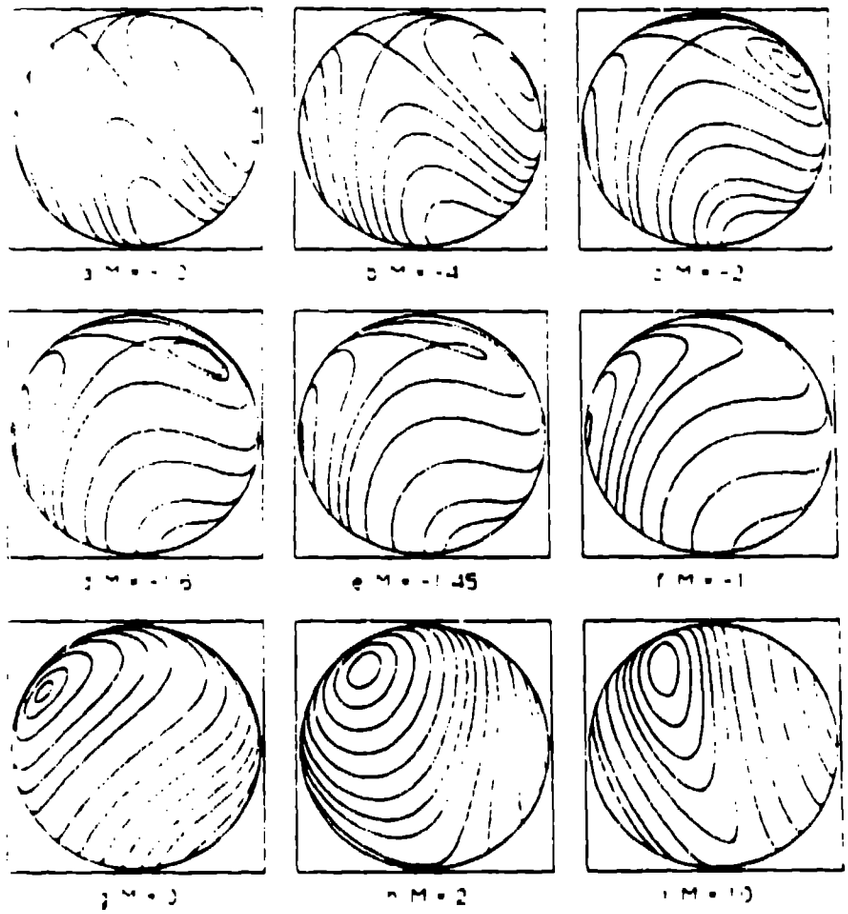

Figure 4.8. Bifurcations for case 6.

5. Homoclinic chaos. In this section, we will use the *Melnikov* technique (see Melnikov [1963, Guckenheimer and Holmes [1983], and Wiggins [1988]) to demonstrate the existence of chaos for our optical system, when the birefringence properties of the propagation medium are perturbed. The important ingredient in this method is the *Melnikov function*, which is defined as follows for a one-degree-of-freedom system. Let H^0 be our previous Hamiltonian function H for the unperturbed system, and let H^1 be the perturbation Hamiltonian. Then the Melnikov function is the line integral of the symplectic Poisson bracket of H^0 and H^1 along an unperturbed homoclinic or heteroclinic orbit and, for our

system, can be written as

$$M(\tau_0) = \int_R \{H^0, H^1\}\,[u(\tau+\tau_0), \phi(\tau+\tau_0)]\,d\tau\ , \tag{5.1}$$

where $u = r\cos\theta$. As discussed in the Introduction, the Melnikov function is a signed measure of the separation (at linear order in perturbation theory) between the *stable* and *unstable* manifolds W^s and W^u, respectively, of the perturbed hyperbolic point; for the unperturbed point these two manifolds coincide, but under various perturbations they may intersect transversely and break up into stochastic layers. *Horseshoe chaos* is the consequence when these manifolds intersect. In particular, transversal intersection in the Poincaré map induces stretching and folding, as a rectangular region of the phase space is mapped away from and then back into the vicinity of the hyperbolic fixed point. These effects are sufficient to cause horseshoe tangles (see Figure 5.1 and Wiggins [1988]).

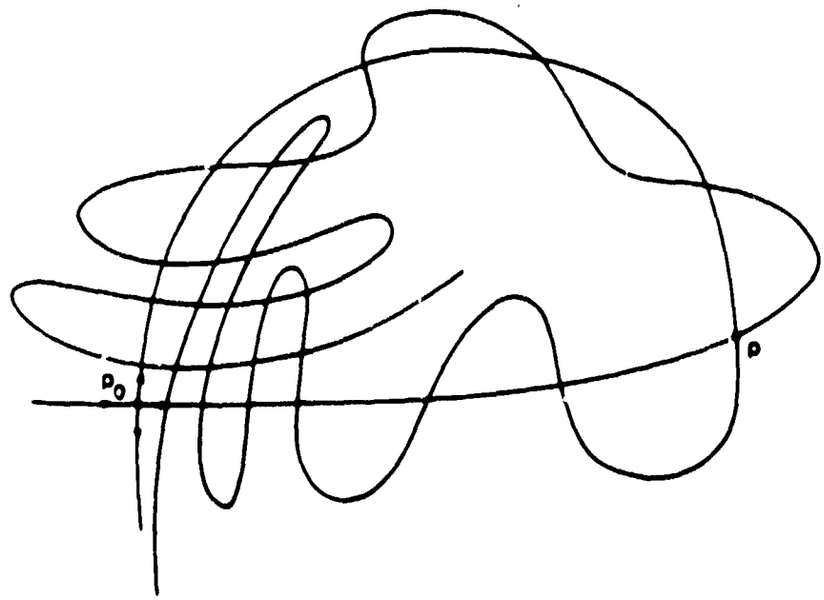

Figure 5.1. Break up of a homoclinic orbit.

The tangles shown in Fig. 5.1 will develop, provided the Melnikov function possesses simple zeroes. The application of the Melnikov technique consists of the following basic

steps. First, one introduces a phase parameter τ_0 which parametrizes the unperturbed homoclinic orbit connected to the hyperbolic fixed point. Then, the bracket $\{H^0, H^1\}$ is constructed and the Melnikov integral is evaluated as a function of τ_0. Finally, one analyzes this function and ascertains whether it has simple zeroes as τ_0 varies, thereby implying the existence of transverse intersections and, thus, horseshoe chaos.

We illustrate the Melnikov procedure for Case 4, in the situation when the north pole is a saddle point connected to a pair of homoclinic loops; we are thus considering regions 2, 5, or 8 in Figure 4.2. In terms of the symplectic variables $u = r\cos\theta$ and ϕ, we can integrate the equations of motion (3.15) along the homoclinic orbit (on the level surface $H^0 = 0$) to get

$$\tan\phi = \tan\phi_o / \tanh(\zeta\tau) , \qquad \zeta = \tfrac{1}{2}\mu r \sin(2\phi_o) ,$$
$$u = -r - \frac{2b_2\left[1 - \cos^2\phi_o \mathrm{sech}^2(\zeta\tau)\right]}{\mu\{\cos^2\phi_o \tanh^2(\zeta\tau) - \lambda\left[1 - \cos^2\phi_o \mathrm{sech}^2(\zeta\tau)\right]\}} . \tag{5.2}$$

where $\mu = \lambda_3 - \lambda_1$. Let us then consider a periodic perturbation of b_2 and λ_2 in the following form:

$$\lambda_2' = \lambda_2 + \epsilon_1 \cos(\nu z) , \qquad b_2' = b_2 + \epsilon_2 \cos(\nu z) , \tag{5.3}$$

where $\epsilon_{1,2} \ll 1$ and ν is the spatial modulation frequency. The Hamiltonian function corresponding to these two periodic perturbative effects is

$$H^1 = \tfrac{1}{2} u\,(\epsilon_1 u + 2\epsilon_2)\cos(\nu z) , \tag{5.4}$$

from which we calculate the Poisson bracket for the Melnikov integrand,

$$\{H^0, H^1\} = -\mu \sin\phi\cos\phi\,(r^2 - u^2)\,u\cos(\nu z) . \tag{5.5}$$

The Melnikov integral defined in Eq. (5.1) then becomes

$$M(\tau_0) = \mu \int_R \sin\phi(\tau)\cos\phi(\tau)[r^2 - u^2(\tau)]\,(\epsilon_1 u(\tau) + \epsilon_2)\cos[\nu(\tau - \tau_0)]d\tau, \tag{5.6}$$

where $\tau_0 = -ct$. In the particular case where $\lambda_2 = \lambda_3$, the Melnikov integral may be evaluated as

$$M(\tau_0) = \frac{2\pi\nu^2}{b_2^2}\left\{r\,(\epsilon_1 r + \epsilon_2) + \tfrac{1}{3}\epsilon_1 r^2\left[\cos^2\phi_o + (\nu/2b_2)^2\right]\right\} \mathrm{csch}\left[\nu\pi/\mu r\sin(2\phi_o)\right]\sin(\nu\tau_0) . \tag{5.7}$$

As a function of τ_0, this expression has simple zeroes, thereby implying horseshoe chaos. As we have been discussing earlier, this means that a region near the homoclinic point at the north pole, under the iteration of the *Poincaré map*, is stretched and folded, and mapped back into itself repeatedly to create a Smale horseshoe. As the horseshoe folds and refolds under the Poincaré map, the self-intersection of a rectangular region initially nearby the homoclinic point develops into a Cantor set structure containing countably many periodic motions, and uncountably many unstable nonperiodic motions. The physical significance of this dynamics is a deterministic, but essentially unpredictable, wandering of the polarization vector to the left or to the right each time the polarization returns to the vicinity of the hyperbolic point at the north pole of the Poincaré sphere.

6. Conclusions. We have studied the dynamics of an optical laser pulse propagating as a travelling wave through a nonlinear polarizable medium. We have seen that the system is reducible to motion on the sphere, in virtue of its invariance under simultaneous phase changes of the two complex electric field amplitudes. The reduced system turns out to be equivalent to a rigid body with a flywheel attachment. We have discovered a rich set of bifurcations in the phase portrait on S^2 as intensity and material parameters are varied, as shown in Figures 4.1 to 4.5. Chaotic behavior under certain classes of spatialy periodic perturbations of the optical medium has also been demonstrated by using the Melnikov method. The horseshoe chaos which occurs corresponds to sensitive dynamics on the Poincaré sphere in the form of an intermittent switching from one elliptical polarization state to another one whose semi-major axis is approximatively orthogonal to that of the first one; the transition between these two states is characterized by a passage nearby the circular state of polarization, once during each switching. Under spatially periodic perturbations of b_2 or W, this switching is very sensitive to initial conditions; the orbits seem to transit randomly from side to side on the Poincaré sphere.

From considerations of the special case in which the Duffing equations (3.16) and (3.17) appear, one could have expected homoclinic chaos to develop for the one-beam travelling-wave problem of nonlinear optical polarization dynamics. The Duffing oscillator is well known to behave chaotically under a large range of perturbations (see, e.g., Wiggins [1988], chapter 4). A related special case of polarization dynamics was studied numerically in Wabnitz [1987]. In contrast to such numerical investigations, our approach is analytical and explores the bifurcations available to the polarization dynamics of the system under

the full range of values for the material parameters, demonstrates that the Smale horseshoe map is the mechanism underlying the chaotic behavior, and characterizes the chaotic set, or stochastic layer as a homoclinic tangle. The strong dependence of the travelling-wave optical polarization dynamics upon the intensity of the beam indicates that control and predictability of optical polarization in nonlinear media may become an important issue for future research. For instance, the sensitivity on initial conditions discussed earlier may well have implications for the control of optical switching in birefringent media. Outlooks for the work presented here include the addition of dissipation and dispersion; this would imply that we could no longer restrict to the regime of travelling waves: we then would have to deal with partial differential equations, i.e., infinite-dimensional dynamical systems, with their attendant new concerns – for example, wave effects, modulational instabilities, and the existence of inertial manifolds. For an introductory example of a partial differential equation system related to the present work for which dynamical system methods have recently made some headway, see Doering *et al.* [1988].

References.

V.I. Arnold [1964], Instability of dynamical systems with several degrees of freedom, Sov. Math. Dokl. **156**, 9–12.

M. Crampin and F.A.E. Pirani [1981], ***Applicable Differential Geometry***, London Mathematical Society Lecture Notes Series **59**, Cambridge University Press, Cambridge (U.K.).

D. David [1989], Horseshoe chaotic dynamics in a polarized optical beam subject to periodic and dissipative perturbations, Preprint, Los Alamos National Laboratory.

D. David, D.D. Holm, and M.V. Tratnik [1988a], Integrable and chaotic polarization dynamics in nonlinear optical beams, Phys. Lett. **137A**, 355–364.

D. David, D.D. Holm, and M.V. Tratnik [1988b], Horseshoe chaos in a periodically perturbed polarized optical beam, Phys. Lett. **138A**, 29–36.

D. David, D.D. Holm, and M.V. Tratnik [1989], Hamiltonian chaos in nonlinear optical polarization dynamics, Physics Reports (in press).

C.R. Doering, J.D. Gibbon, D.D. Holm, and B. Nicolaenko [1988], Low dimensional behaviour in the complex Ginzburg Landau equation, Nonlinearity 1, 279–309.

A.L. Gaeta, R.W. Boyd, J.R. Ackerhalt, and P.W. Milonni [1987], Instabilities and chaos in the polarizations of counterpropagating light fields, Phys. Rev. Lett. **58**, 2432–2435; Instabilities in the propagation of arbitrarily polarized counterpropagating waves in a nonlinear Kerr medium, in *Optical Bistability III*, H.M. Gibbs, P. Mandell, N. Peyghambarian, S.D. Smith (eds.), Springer-Verlag, Berlin.

B. Greenspan and P.J. Holmes [1981], Homoclinic orbits, subharmonics, and global bifurcations in forced oscillations, in: *Nonlinear Dynamics and Turbulence*, G. Baranblatt, G. Iooss, D.D. Joseph (eds.), Pitman.

J. Guckenheimer and P.J. Holmes [1983], *Nonlinear Oscillations, Dynamical Systems, and Bifurcations of Vector Fields*, Applied Mathematical Sciences, Vol. **42**, Springer-Verlag, New-York.

D.D. Holm, J.E. Marsden, T. Ratiu, and A. Weinstein [1985], Nonlinear stability of fluid and plasma equilibria, Physics Reports **123**, 1–116.

P.J. Holmes and J.E. Marsden [1982], Horseshoes in perturbations of Hamiltonian systems with two degrees of freedom, Comm. Math. Phys. **82**, 523–544.

A.E. Kaplan [1983], Light-induced nonreprocity, field invariants, and nonlinear eigenpolarizations, Opt. Lett. **8**, 560–562.

R. Lytel [1984], Optical multistability in collinear degenerate four-wave mixing, J. Opt. Soc. Am. **B1**, 91–94.

P.D. Maker, R.W. Terhune, and C.M. Savage [1964], Intensity-dependent changes in the refractive index of liquids, Phys. Rev. Lett. **12**, 507–509.

V.K. Melnikov [1963], On the stability of the center for time periodic perturbations, Trans. Moscow Math. Soc. **12**, 1–57.

K. Otsuka, J. Yumoto, and J.J. Song [1985], Optical bistability based on self-induced polarization-state change in anisotropic Kerr-like media, Opt. Lett. **10**, 508–510.

M.V. Tratnik and J.E. Sipe [1987], Nonlinear polarization dynamics. I. The single-pulse equations, Phys. Rev. **A35**, 2965–2975; II. Counterpropagating beam equations: new simple solutions and the possiblity for chaos, Phys. Rev. **A35**, 2976–2988; III. Spatial polarization chaos in counterpropagating beams, Phys. Rev. **A36**, 4817–4822.

S. Wabnitz [1987], Spatial chaos in the polarization for a birefringent optical fiber with periodic coupling, Phys. Rev. Lett. **58**, 1415–1418.

S Wiggins [1988], ***Global Bifurcations and Chaos - Analytical Methods***, Applied Mathematical Sciences **73**, Springer–Verlag, New York.